https://doi.org/10.1093/plcell/koac089 THE PLANT CELL 2022: 34: 2328–2342

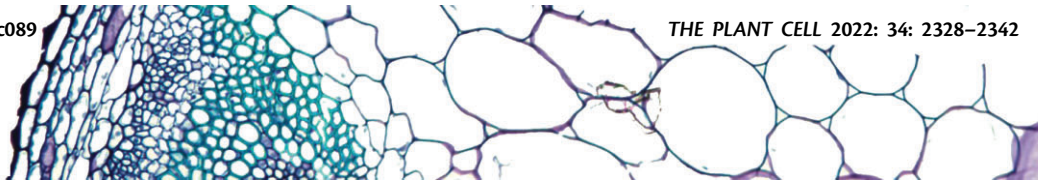

Research Article

Out of the blue: Phototropins of the leaf vascular bundle sheath mediate the regulation of leaf hydraulic conductance by blue light

Yael Grunwald [1], Sanbon Chaka Gosa [1], Tanmayee Torne-Srivastava [1], Nava Moran [1] and Menachem Moshelion [1,*,†]

1 The Robert H. Smith Institute of Plant Sciences and Genetics in Agriculture, The Robert H. Smith Faculty of Agriculture, Food and Environment, The Hebrew University of Jerusalem, Rehovot 76100, Israel

*Author for correspondence: menachem.moshelion@mail.huji.ac.il
These authors contributed equally (Y.G. and S.C.G.).
†Senior author

Y.G. and S.C.G. preformed all molecular work including vector construction and plant transformation, planned and performed the K_{leaf} and vein pH experiments, and wrote the paper. Y.G. planned and performed the P_f experiments. T.T. planned and performed the membrane potential and cytosolic pH experiments. N.M. and M.M. conceptualized and supervised the project and wrote the paper.
The author responsible for distribution of materials integral to the findings presented in this article in accordance with the policy described in the Instructions for Authors (https://academic.oup.com/plcell) is Menachem Moshelion (menachem.moshelion@mail.huji.ac.il).

Abstract

The Arabidopsis (*Arabidopsis thaliana*) leaf veins bundle-sheath cells (BSCs)—a selective barrier to water and solutes entering the mesophyll—increase the leaf radial hydraulic conductance (K_{leaf}) by acidifying the xylem sap by their plasma membrane H^+-ATPase, AHA2. Based on this and on the BSCs' expression of phototropins *PHOT1* and *PHOT2*, and the known blue light (BL)-induced K_{leaf} increase, we hypothesized that, resembling the guard cells, BL perception by the BSCs' phots activates its H^+-ATPase, which, consequently, upregulates K_{leaf}. Indeed, under BL, the K_{leaf} of the knockout mutant lines *phot1-5*, *phot2-1*, *phot1-5 phot2-1*, and *aha2-4* was lower than that of the wild-type (WT). BSC-only-directed complementation of *phot1-5* or *aha2-4* by *PHOT1* or *AHA2*, respectively, restored the BL-induced K_{leaf} increase. BSC-specific silencing of *PHOT1* or *PHOT2* prevented such K_{leaf} increase. A xylem-fed kinase inhibitor (tyrphostin 9) replicated this also in WT plants. White light—ineffective in the *phot1-5* mutant—acidified the xylem sap (relative to darkness) in WT and in the *PHOT1*-complemented *phot1-5*. These results, supported by BL increase of BSC protoplasts' water permeability and cytosolic pH and their hyperpolarization by BL, identify the BSCs as a second phot-controlled water conductance element in leaves, in series with stomatal conductance. Through both, BL regulates the leaf water balance.

Introduction

Light, the energy source for photosynthesis, also regulates plant growth and development (Kronenberg and Kendrick, 1986) as well as physiological traits such as stomatal conductance (g_s; Zeiger and Helper, 1977; Karlsson, 1986; Talbott et al., 2003) and leaf hydraulic conductance (K_{leaf}; Voicu et al., 2008; Ben Baaziz et al., 2012; Aasamaa and Sõber, 2012; Prado and Maurel, 2013). One of the most conserved and well-studied light-sensing mechanisms is the sensing of blue light (BL; 390–550 nm) that causes stomata to open

Received June 09, 2021. Accepted March 10, 2022. Advance access publication March 14, 2022

IN A NUTSHELL

Background: Plants sense and react to their environment in a variety of ways. As an example, blue light (BL) causes the opening of stomata and increases fluid flow in the vascular system (by increasing the leaf conductance to water, K_{leaf}). K_{leaf} is regulated by a tight cell layer (bundle-sheath cells [BSCs]) that surrounds the entire vascular system (like a sleeve). We have recently discovered that two BL receptor proteins, phot1 and phot2, which are an important part of the BL sensory system, are also located in the BSCs. These receptors respond even to low intensities of BL.

Question: We asked whether BL regulates K_{leaf} through the phot1 and phot2 photoreceptors of the BSCs. Furthermore, what is their mechanism of action and is it similar to the one that activates the stomatal guard cells' response to BL?

Findings: The BL photoreceptors phot1 and phot2, located in the BSCs, play an important role in regulating K_{leaf} in the model plant Arabidopsis's vascular system. When BL hits these photoreceptors, it initiates a signal transduction pathway (a series of biochemical events) that activates proton pumps in the BSC membranes, which pump protons into the xylem, making the xylem sap more acidic. This acidification increases the BSCs' permeability to water, which increases the water flow in the entire leaf.

Next step: Since plants "trade" water for the CO_2 they assimilate photosynthetically, understanding how leaves regulate their water balance in response to stress hormones, such as abscisic acid, may help us create plants that are more drought resistant and more photosynthetically efficient. We intend to study this mechanism in crop plants in the future and to use genetic manipulations to extend the time that plants are able to assimilate CO_2 even under stressful conditions.

(Grondin et al., 2015). In this signal transduction pathway in the guard cells (GCs), BL is perceived by the protein kinases phot1 and phot2 (Kinoshita et al., 2001). Their immediate phosphorylation substrate is Blue Light Signaling1 (BLUS1; At4g14480; Takemiya et al., 2013), which is a part of the earliest stomata-opening BL signaling complex with phot. Another part of this complex is the Raf-like kinase, BL-dependent H^+-ATPase phosphorylation (BHP), At4g18950; Hayashi et al., 2017; reviewed by Inoue and Kinoshita, 2017). While none of these directly phosphorylates the GC H^+-ATPase (Hayashi et al., 2017), one of the other Raf-like kinases downstream of phot could be the target of tyrphostin 9 (TP9), a kinase inhibitor that has been shown to inhibit the BL-induced phosphorylation of the penultimate threonine of the plasma membrane H^+-ATPase (Arabidopsis H^+ATPase (AHA)) in Arabidopsis GCs (Hayashi et al., 2017). This BL-induced phosphorylation activates the AHA (Kinoshita and Shimazaki, 1999; Svennelid et al., 1999), which, in turn, hyperpolarizes the GCs and acidifies their surrounding apoplast (Kinoshita and Shimazaki, 1999; Ueno et al., 2005; Den Os et al., 2007; Elmore and Coaker, 2011, reviewed by Inoue and Kinoshita, 2017). Conversely, at night, in the dark, the GCs' H^+-ATPases are deactivated, the GCs are depolarized, and their apoplast becomes alkaline (Kinoshita and Shimazaki, 1999; Kinoshita et al., 2001). These pH and membrane potential changes cause ion and water fluxes across the GCs' membranes causing their osmotic swelling during the day and shrinking at night, which underlies stomata opening and closure (Assmann, 1993; Roelfsema and Hedrich, 2005; Shimazaki et al., 2007).

Both BL and white light (WL) have been shown to increase the hydraulic conductance (K_{leaf}) of the entire leaf in several plant species [(Voicu et al., 2008 (bur oak, *Quercus macrocarpa*); Voicu et al., 2009; Sellin et al., 2011 (silver birch, *Betula pendula* Roth); Aasamaa and Sober, 2012 (deciduous trees); Ben Baaziz et al., 2012 (walnut, *Juglans regia* L.)]. Interestingly, K_{leaf} responds more quickly to light than g_s does (Guyot et al., 2012). However, the molecular mechanism by which K_{leaf} increases in response to light quality is not yet fully understood.

In the past decade, it has been established that bundle-sheath cells (BSCs), which form a parenchymal layer that tightly enwraps the entire leaf vasculature, can act as a dynamic and selective xylem–mesophyll barrier to water and ions, and participate in K_{leaf} regulation (Shapira et al., 2009; Shatil-Cohen and Moshelion, 2012). Moreover, we recently discovered that the BSCs' H^+-ATPase proton pump, AHA2, participates in regulating K_{leaf} via changes in the xylem pH and that the positive correlation observed between AHA2-driven xylem acidification and K_{leaf} is due to an increase in the osmotic water permeability of BSCs' membranes (Grunwald et al., 2021). AHA2 is particularly abundant in BSCs (present at more than three-fold higher level than that seen in neighboring mesophyll cells; Wigoda et al., 2017), which explains how such acidification is possible. In addition, the same BSC transcriptome analysis (Wigoda et al., 2017) revealed substantial expression of the BL receptors phot1 and phot2 in BSCs, as well as substantial expression of the kinases BHP and BLUS1. These findings led us to hypothesize that the vascular BSCs possess a BL signal transduction pathway that is similar to the one that opens stomata and that plays a role in the regulation of K_{leaf}. In support of this hypothesis, we describe here a few of the physiological and molecular mechanisms underlying the BL-dependent regulation of K_{leaf} by BSCs.

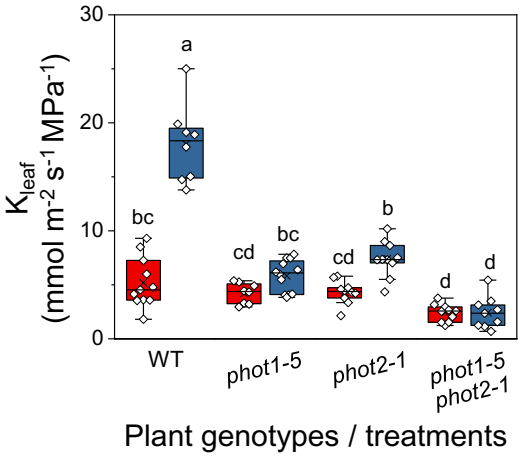

Figure 1 The effect of BL on the K_{leaf} of PHOT receptor mutants. K_{leaf} of fully expanded, excised leaves of WT (Col-gl) and *PHOT* mutants [*phot1-5* (Col-gl), *phot2-1* (Col-gl), and a double mutant, *phot1-5 phot2-1* (Col-gl)] determined immediately after 15 min of illumination with RL (left red boxes; 220 µmol m^{-2} s^{-1}) or RL + BL (right blue boxes; 220 µmol m^{-2} s^{-1}, consisting of 90% RL and 10% BL). The box height delimits 25%–75% of the data range. Symbols represent the individual data values, solid lines indicate the median, and × indicates the mean. The whiskers delimit ±1.5 times the inter-quartile range. Different letters indicate statistically different means (analysis of variance (ANOVA), Tukey's honest significant difference (HSD) test, $P < 0.05$). Note the reduced response to RL + BL in the mutant lines.

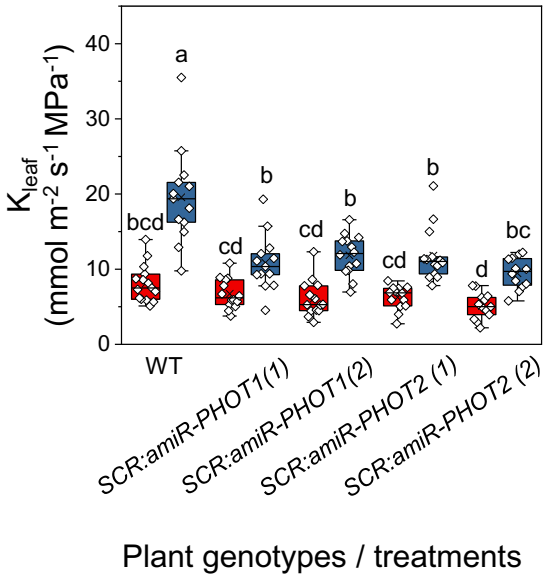

Figure 2 *amiR*-silencing of *PHOT1* or *PHOT2* (*SCR:amiR-PHOT* plants) in the BSCs reduces K_{leaf} under RL + BL light. K_{leaf} was determined in fully expanded leaves of WT, *SCR:amiR-PHOT1* (two independent lines 1 and 2) and *SCR:amiR-PHOT2* (two independent lines 1 and 2) plants treated with RL or RL + BL (as in Figure 1). Other details are also as in Figure 1.

Results

phot1 and phot2 BL receptors are involved in the regulation of K_{leaf}

Following the GC model in which the photoreceptors phot1 and phot2 transduce the BL stomatal-opening signal, and encouraged by the substantial expression of the BL receptor genes *PHOT1* and *PHOT2* in the transcriptome of Arabidopsis BSCs (Wigoda et al., 2017), we explored the roles of these two light receptors in the regulation of hydraulic conductance (K_{leaf}). We compared the K_{leaf} of wild-type (WT) plants to the K_{leaf} of knockout mutants lacking one or both light receptors (*phot1-5*, *phot 2-1*, and *phot1-5 phot 2-1*; Figure 1) under two light regimes, red light (RL) and RL + BL. Under RL + BL, the K_{leaf} of WT leaves was more than three-fold higher than it was under RL treatment and more than two-fold higher than the K_{leaf} values of the three mutants treated with RL + BL. Also, under RL + BL, the K_{leaf} of the *phot2-1* mutant was ∼40% higher than it was under the RL treatment. In contrast, BL did not seem to increase the K_{leaf} of the *phot1-5* mutant or that of the double mutant. Under RL, there were no differences between the K_{leaf} levels of the different mutants. However, while the WT's K_{leaf} was no different from that of the single mutants, it was about double than that of the double mutant (Figure 1). The BL response was particularly depressed in the double mutant: only 13% of the WT's K_{leaf} BL response remained in the double mutant, as compared to 32% and 40% of the WT's K_{leaf} in *phot1-5* and in *phot2-1*, respectively (Figure 1), and only 35% of the WT's g_s BL response remained in the double mutant, as compared to 57% and 71% of the WT's g_s in *phot1-5* and *phot2-1*, respectively (Supplemental Figure S1A).

The higher calculated K_{leaf} value of the WT under BL (as compared to RL) was due to a greatly increased (less negative) leaf water potential (Ψ_{leaf}) and an appreciably higher transpiration rate (E; Equation 1, "Materials and methods"). This invites the interpretation that the BL induced a highly conductive water pathway into the leaf, enabling higher radial water influx which, in turn, was able to compensate for the BL's enhancement of E (i.e. water efflux from the leaf via the BL-increased g_s; Supplemental Figure S1).

BSC-specific silencing of phot1 and phot2 receptors decreased K_{leaf}

To examine the specific participation of the BSCs' light receptors in the BL-induced increase in K_{leaf}, we silenced either the *PHOT1* or the *PHOT2* gene using artificial microRNA (amiRNA) under the BSC-specific promoter, *SCARECROW* (*SCR*, see "Materials and methods"). Under RL + BL illumination, the K_{leaf} values of leaves of both types of transgenic plants, *SCR:amiR-PHOT1* and *SCR:amiR-PHOT2*, were lower than the K_{leaf} values of the WT leaves (by 40%–50%; Figure 2). In contrast, all of the *SCR:amiR-PHOT* plants had WT-like g_s and E, while their Ψ_{leaf} levels were lower than that of the WT (by 50%–90%), suggesting a reduction

in the radial influx of water into the leaf (Supplemental Figure S2).

BSC-specific complementation of the *phot1-5* mutant with *PHOT1* restored K_{leaf}

We complemented the *phot1-5* (Col-gl) mutant plants with *SCR:PHOT1* to restore phot1 activity exclusively in the BSCs (see "Materials and methods") and compared them to WT (Col-gl) plants and to *phot1-5* plants. *SCR:PHOT1* plants illuminated with RL + BL had their K_{leaf} restored from *phot1-5* values to WT levels (Figure 3). While, as expected, BL increased the WT's g_s, the mutant's g_s and the g_s of the complemented mutant did not change under BL, also as expected from the main BL-receptor-devoid GCs (Supplemental Figure S3). Under BL, the Ψ_{leaf} of the *SCR:PHOT1*-complemented mutant was restored to the WT level and both of those values were >50% greater than the mutant's Ψ_{leaf} (Supplemental Figure S3). Thus restored Ψ_{leaf} was the major contribution to the restored high K_{leaf} of the complemented mutant, suggesting a restoration of radial water influx to the leaf.

The kinase inhibitor, TP9, prevented the increase in K_{leaf} under BL

The kinase inhibitor TP9 suppresses BL-dependent H^+-ATPase phosphorylation (of the penultimate threonine) in GCs (Hayashi et al., 2017). To examine further whether the vascular phot receptors initiate a similarly sensitive phosphorylating event in the BL-dependent K_{leaf} regulation pathway, we perfused detached WT leaves with artificial xylem solution (AXS), with or without 10μM TP9, and exposed them to RL or RL + BL. The K_{leaf} values of RL + BL-illuminated leaves perfused with TP9 were ~50% lower than those of RL + BL-illuminated control leaves (without TP9) and were no different than the K_{leaf} of leaves illuminated with only RL (with or without exposure to TP9; Figure 4A, Xylem fed, on the left, Supplemental Figure S4). However, g_s was not affected by the petiole-delivered TP9 (Figure 4B, left). In contrast to the perfused TP9, spraying the inhibitor on the leaf surface did not interfere with the almost threefold increase in K_{leaf} that was induced by BL (Figure 4A, right), but it did prevent the BL-induced increase in g_s (Figure 4B, Sprayed, on the right). The impaired stomatal response as a result of the application of TP9 directly to the leaf surface is in agreement with TP9's previously reported inhibition of BL-induced stomatal opening in epidermal peels (Hayashi et al., 2017). Leaf transpiration, E, behaved in

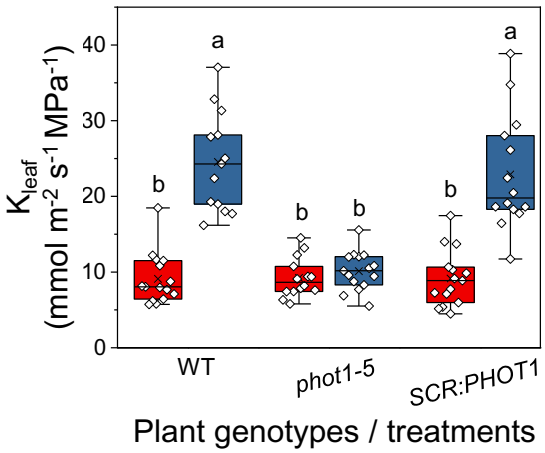

Figure 3 BSC-directed *PHOT1* complementation of the *phot1-5* mutant restores the normal K_{leaf}. Fully expanded leaves of WT (Col-gl), *phot1-5* (Col-gl), and *phot1-5* (Col-gl) plants complemented with *SCR:PHOT1* were subjected to illumination treatments, as in Figure 1. Other details are also as in Figure 1.

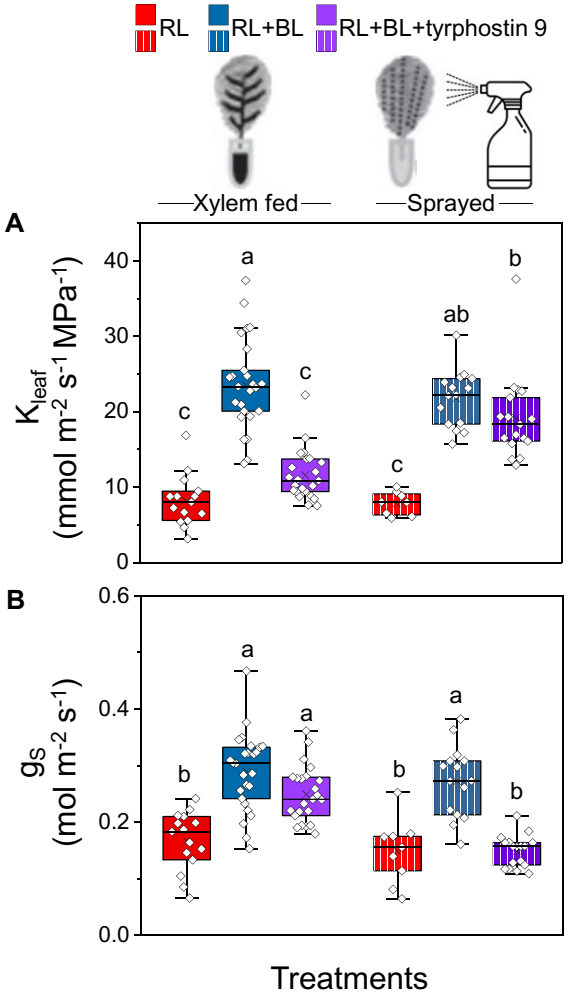

Figure 4 The kinase inhibitor TP9 either abolished the BL-induced K_{leaf} increase or prevented the BL-induced stomatal opening, depending on the treatment route. Fully expanded leaves of WT (Col-gl) were preincubated (petiole deep) in AXS without or with TP9 (10 μM) or sprayed with AXS with or without TP9 (10 μM) and kept overnight in dark boxes. Immediately after the dark treatment, leaves were illuminated for 15 min with RL or RL + BL, as indicated. A, K_{leaf}. B, Stomatal conductance (g_s). Other details are as in Figure 1. Note that K_{leaf} was reduced when TP9 was fed via the petiole, but not when it was sprayed on the plants, and that the opposite was true for g_s.

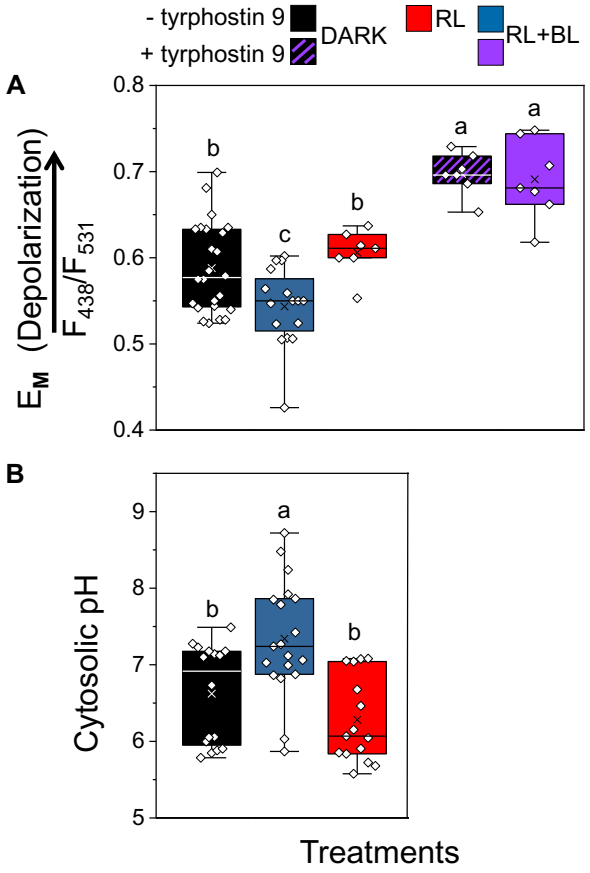

Figure 5 BL hyperpolarizes the isolated BSC protoplasts and alkalinizes their cytosol relative to RL or darkness, and TP9 depolarizes them. A, Membrane potential (E_M, in units of the fluorescence ratio) of BSC protoplasts, with or without bath-added TP9 (10 μM), determined using the dual-excitation, ratiometric fluorescent dye di-8-ANEPPS. After at least 10 min in the dark, the cells were immediately imaged (dark treatment) or illuminated for an additional 5–10 min either with RL or RL + BL and then imaged ("Materials and methods"). The symbols represent the mean fluorescence ratio (F_{438}/F_{531}, *F*-ratio) values from individual protoplasts (biological repeats), derived from analysis of their images captured at the indicated excitation wavelengths in three to eight independent experiments. The positive correlation between E_M and the *F*-ratio (with depolarization indicated by the arrow) was verified in separate experiments using patch clamp (Supplemental Figure S6). Different letters denote significantly different values (ANOVA, post hoc Tukey's test; $P < 0.05$). Other box plot details are as in Figure 1. B, pH_{CYT} of BSC protoplasts determined using the fluorescent dual-emission pH probe SNARF1. Protoplasts were dark-treated for 10 min and then further treated with 10 min of either dark, RL or RL + BL, and then imaged. pH_{CYT} values were derived from the analysis of the captured pairs of images of individual protoplasts (biological repeats); the emitted fluorescence ratio (F_{640}/F_{585}) values were converted to pH values based on a calibration curve (as detailed in Torne-Srivastava et al., 2021). The data are from at least three independent experiments. Other details are as in (A).

a pattern similar to g_s (Supplemental Figure S5A). Petiole-fed TP9 abolished the BL-induced increase in Ψ_{leaf}, but TP9 sprayed on the leaf surface did not prevent it (Supplemental Figure S5B).

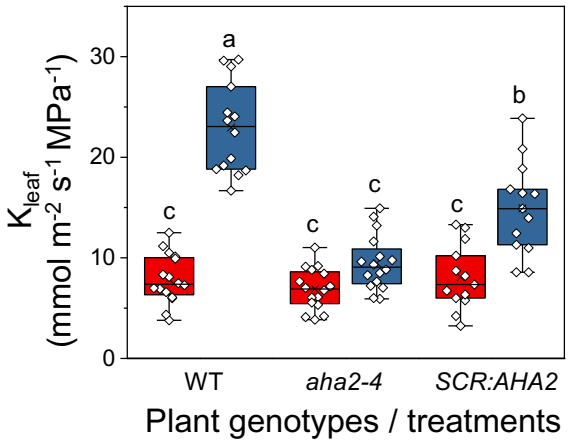

Figure 6 The BSC H^+-ATPase, AHA2, mediates the BL-induced increase in K_{leaf}. Fully expanded excised leaves of WT (Col-0) plants, *aha2-4* mutant plants (Col-0), and *aha2-4* plants complemented in their BSCs with *SCR:AHA2* were illuminated for 15 min immediately after the dark treatment, as in Figure 1. The box-plot details are also as in Figure 1. Note the marked restoration of K_{leaf} in the *aha2* mutant plants complemented solely in their BSCs.

BL hyperpolarizes the BSCs and raises their cytosolic pH

To investigate further whether the BSCs' BL signal transduction pathway stimulates their plasma membrane H^+-ATPases (as in GCs), we monitored the membrane potential of BSC protoplasts using the potentiometric dual-excitation dye di-8-ANEPPS. Indeed, 5–10 min of RL + BL illumination hyperpolarized the BSC protoplasts relative to RL alone or to the dark (absence of illumination), while 10-μM TP9 added in the bath depolarized the BSCs irrespectively of RL + BL illumination or its absence (Figure 5A; Supplemental Figure S6), hence, apparently independently of the inhibition of AHA activity.

To further explore our hypothesis of H^+-ATPase activation by BL, we monitored the cytosolic pH (pH_{CYT}) using the ratiometric, dual-emission fluorescent pH-sensitive dye, SNARF1. The pH_{CYT} of BSCs illuminated for 10 min with RL + BL (following dark treatment) was significantly more alkaline (by 0.72 pH units) than the pH_{CYT} of dark-treated BSCs and 1.06 pH units higher than the pH_{CYT} of the BSCs that were treated with only RL (Figure 5B), consistent with BL-induced activity of H^+-ATPases, which move protons from the BSCs into the xylem.

AHA2 plays a role in the BL-induced regulation of K_{leaf}

Recently, we reported that AHA2 plays a major role in K_{leaf} regulation by acidifying the xylem sap. To further examine whether the BSCs' H^+-ATPase AHA2 participates in the *BL-initiated* K_{leaf} regulation, we examined the AHA2 knockout mutant *aha2-4* and its BSC-complemented transgenic plant line *SCR:AHA2* (i.e. the *aha2-4* mutant with AHA2 expressed

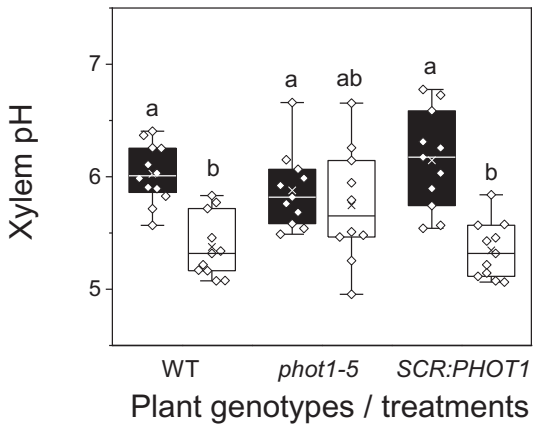

Figure 7 Illumination with WL for 30 min acidified the xylem pH of WT plants and *SCR:PHOT1*-complemented mutants, but not that of the *phot1-5* mutant. The leaves of WT (Col-gl) plants, *phot1-5* (Col-gl) mutants, and the *SCR:PHOT1*-complemented *phot1-5* mutant (as in Figure 3) were illuminated with WL in the growth room (150–200 µmol m^{-2} s^{-1}). Black boxes indicate dark and empty boxes indicate WL. Other box plot details are as in Figure 1.

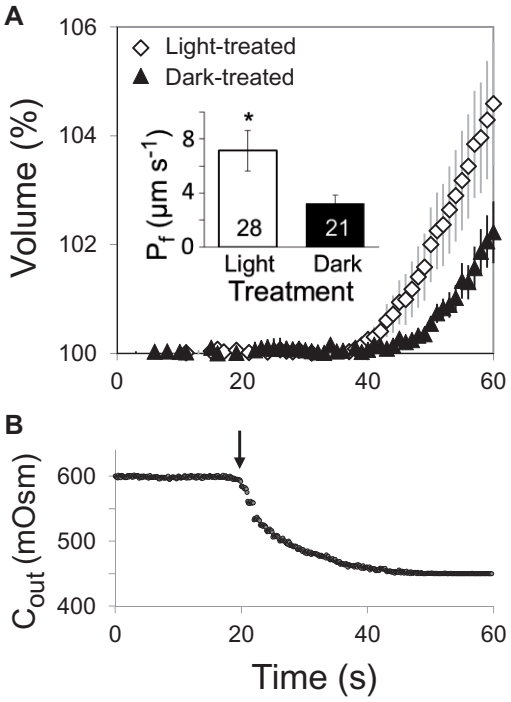

Figure 8 WL increases the BSCs' membrane osmotic water permeability coefficient (P_f). A, Time course of the swelling (mean relative volume ±SE versus time) of *n* bundle-sheath protoplasts from *SCR:GFP* plants upon exposure to a hypotonic solution under the same illumination conditions (WL or darkness) as during the light treatment preceding the assay ("Materials and methods"). Inset: the mean (±SE) initial P_f values of the indicated number (*n*) of BSC protoplasts under two illumination regimes from five independent experiments. The asterisk indicates a significant difference (at $P < 0.05$; Student's two-tailed, nonpaired *t* test). B, Time course of the osmotic concentration change in the bath (C_{out}) during the hypotonic challenge; the arrow indicates the onset of the bath flush ("Materials and methods").

only in its BSCs; Grunwald et al., 2021) under the two light regimes (RL and RL + BL). The K_{leaf} of *aha2-4* leaves did not respond to the RL + BL illumination and was only ∼40% of the K_{leaf} of BL-treated WT leaves. However, similar illumination increased the K_{leaf} of the AHA2-complemented (*SCR:AHA2*) plants to almost 65% of the WT's K_{leaf} (Figure 6), indicating that the BL-induced increase in K_{leaf} is dependent on AHA2. In contrast, under RL + BL, the E and g_s of *SCR:AHA2* did not differ from the E and g_s of the *aha2-4* mutant, and they remained unaffected by BL and lower than the E and g_s of the WT (Supplemental Figure S7, A and B). Notably, the Ψ_{leaf} of *SCR:AHA2* was ∼40% higher than the Ψ_{leaf} of *aha2-4* and did not differ from that of the WT, suggesting a restoration of radial water influx to the leaf (Supplemental Figure S7C).

Morning light after night darkness acidifies the xylem sap

To delve further into the acidification-mediated link between light and K_{leaf}, we explored the diurnal transition between the xylem sap pH in the night and in the morning. We hypothesized that the xylem sap pH would be reflected in the pH of guttation drops exuded via hydathodes from the ends of the xylem conduits. Therefore, to take a preliminary peek at the xylem sap pH at night, we measured the pH of guttation drops collected from the tips of WT leaves before the lights were turned on and found that their mean pH was 7.2 ± 0.04 (standard error (±SE), 15 biological repeats collected over 3 days). Next, we measured the pH of the xylem sap in detached leaves, comparing leaves before dawn to leaves after dawn (i.e. leaves at the end of an overnight dark treatment to leaves after a 30 min illumination with WL in the growth chamber). This comparison included leaves of WT, *phot1-5*, and *SCR:PHOT1* plants. Illumination acidified the xylem sap in WT plants by ∼0.6 pH units (from 6.0 to 5.4) and in the *SCR:PHOT1* plants by ∼0.8 pH units (from 6.1 to 5.3), while the xylem pH in *phot1-5* remained unchanged, at ∼5.9 (Figure 7), suggesting that phot1 in the BSCs is necessary for light-activated xylem acidification, which, in turn, increases K_{leaf} (Grunwald et al., 2021).

Light increases the osmotic water permeability, P_f, of the BSCs

To explore the link between light and K_{leaf} at the cellular level, we tested whether light affects the osmotic water permeability (P_f) of the BSC membrane. We determined the P_f of isolated BSC protoplasts from videotapes of their swelling during a hypotonic challenge after illumination with WL or after 10 min in the dark. The illuminated BSCs had higher P_f than the dark-treated ones (Figure 8), suggesting that the morning increase in the movement of water from the xylem to the BSCs (and then, presumably, further into the

mesophyll) is due to increased permeability of the BSC membranes to water.

Leaf vein density is not affected by the expression of phot1 or phot2

To resolve whether the diminished K_{leaf} of the phot receptor mutants that we observed under BL was due to differences in leaf vein density, we quantified the vein density of all of the genotypes that we studied and found no differences among them (Supplemental Figure S8).

Discussion

BL signal transduction in BSCs is reflected in the K_{leaf} increase

We demonstrate here an autonomous BL signaling mechanism in Arabidopsis BSCs that underlies the light-induced increase of K_{leaf}, resembling the "classical" short-term, BL-induced signaling pathway for stomatal opening mediated by the photoreceptors phot1 and phot2 (Zeiger et al., 1983; Kinoshita et al., 2001; Sakai et al., 2001). To explain the underlying mechanism, we built on our earlier findings that the receptor genes *PHOT1* and *PHOT2* are substantially expressed in BSCs (Wigoda et al., 2017; Supplemental Table S2). Here, we link these findings using the phot receptor mutants *phot1-5* and *phot2-1* and the double mutant *phot1-5 phot2-1*. Based on the complete abolishment of the BL-K_{leaf} response (relative to RL alone) in the *phot1-5* mutant, which is presumed to possess phot2 activity, phot2 would appear completely redundant, were it not for (1) the strong depression of the BL-K_{leaf} response—compared to WT response—in the *phot2-1* mutant, presumed to possess phot1 activity and (2) even more severe impairment of the double mutant's BL-K_{leaf} response compared to the responses of both single mutants (Figure 1).

Also the BL-g_s responses that we observed in the three phot mutants were depressed to different relative degrees resembling the gradation of BL-K_{leaf} responses (Supplemental Figure S1A) and suggesting a similar dependence of BL signaling on phots in the two systems (BSCs and GCs). Interestingly, after 2-4 h of illumination (well beyond our usual 20 min of illumination) the *phot* single mutants' g_s re-acquired the WT-like sensitivity to BL (Supplemental Figure S9), similar to an earlier report on stomatal aperture after 2-4 h of illumination with BL (Kinoshita et al., 2001). This could perhaps reflect a gradually accumulating effect of the GCs' AHA activity, overcoming the partially impaired phot-to-AHA signal transduction in the single *phot* mutants.

That the phots (and particularly phot1) are indispensable to BL signaling in the BSCs, as they are in GCs (Kinoshita et al., 2001), is additionally emphasized by our two BSC-delimited genetic phot manipulations: (1) the severe impairment of the BL-induced K_{leaf} increase in WT plants in which either phot1 or phot2 was silenced by the respective *SCR:amiR-PHOT* (Figure 2) and (2) the full restoration of K_{leaf} sensitivity to BL by *phot1-5* complementation with *SCR:PHOT1* (Figure 3). These manipulations, which did not affect g_s (Supplemental Figures S2A and S3A), also emphasize the independence of the BSCs' BL signal transduction from that of the GCs.

Prompted by finding *BLUS1*, which encodes the phots' indispensable partner kinase in the BL-induced early-signaling complex of GCs (Takemiya et al., 2013; Hayashi et al., 2017), also in the BSC's transcriptome (Wigoda et al., 2017; Supplemental Table S2), we found that the *blus1* mutant's K_{leaf} does not respond to BL (Supplemental Figure S10), underscoring further the resemblance in BL signaling between the two systems.

Additionally, the tissue-localized effects of the kinase inhibitor, TP9, which presumably inhibited a BL-signaling kinase downstream of phot-BLUS1, demonstrated both the similarity between the BSCs' and the GCs' BL signaling pathways in WT plants, and, again, the independence of the two systems. Both signaling pathways were inhibited by TP9, but only when it was applied in close proximity to the target tissue: the BSC system was affected only by the petiole-fed TP9, which inhibited the BL-induced increase of K_{leaf} and Ψ_{leaf} without affecting g_s; whereas the GC system was affected only when TP9 was sprayed on the leaf surface (i.e. on GCs), which abolished the BL-induced g_s increase without affecting K_{leaf} (Figure 4; Supplemental Figure S5). Notwithstanding the above, the depolarization of BSCs by TP9 both under RL + BL and in the dark (Figure 5A), suggests an additional or an alternative underlying mechanism outside the AHA-activating BL-signaling pathway.

Recently, we reported that the BSC H^+-ATPase AHA2 plays a major role in the acidification of the xylem sap, which, in turn, increases K_{leaf} (Grunwald et al., 2021). Indeed, the H^+-ATPase mutant *aha2-4* had a diminished (compared to WT) BL-induced increase in K_{leaf} (Figure 6; likely due to a more alkaline xylem pH; Grunwald et al., 2021), as well as a diminished BL-induced increase in g_s (Supplemental Figure S7). In contrast, *aha2-4* plants complemented with the *SCR:AHA2* — even though directed only to BSCs—had their BL-induced K_{leaf} increase restored (Figure 6), while their g_s remained unaffected (Supplemental Figure S7), affirming the importance of the BSC AHA2 in mediating the BL-induced increase in K_{leaf} independently of g_s (i.e. of GCs).

Thus, with the genetic manipulation of the BL receptors phot1 and phot2 in the BSCs, the tissue-differential responses to pharmacological treatment and genetic manipulation of the AHA2, we demonstrated the independence of the BSCs' BL signaling from the GCs' BL signaling. This notion of independence is particularly important since the BSC layer constitutes a hydraulic valve between the xylem and the leaf, regulating water loss to the atmosphere in series with stomatal apertures.

BL signal transduction in BSCs is reflected in their H^+-ATPase activation

Four of our findings focus on the activation of H^+-ATPase as the end-point of BL signaling: at the level of single

isolated BSCs, (1) the BL-induced alkalinization of the BSCs cytosol (relative to dark or to RL; Figure 5B), (2) the BL-induced hyperpolarization in WT (Col) BSC protoplasts (relative to dark or to RL, Figure 5A), and also in WT (Col-gl) BSC protoplasts (Supplemental Figure S11A, "Materials and methods"), (3) the absence of hyperpolarization under RL + BL treatment in the BSC protoplasts of the *phot1-5* mutant and its restoration in the *phot1-5* mutant complemented with *PHOT1* solely in its BSCs (Supplemental Figure S11B); at the level of the detached leaf, (4) acidification of the xylem sap by WL (relative to dark) in WT, the absence of the WL response in the *phot1-5* mutant and a restoration of this response in the abovementioned *PHOT1*-complemented mutant (Figure 7). Taken together, both types of the pH responses (which occur by proton extrusion from the cytosol) and the hyperpolarization (which could also result from proton extrusion via the plasma membrane), resembling the hyperpolarization of GCs in response to BL (Assmann et al., 1985; Roelfsema et al., 2001), are strong evidence linking the phot receptors with the BL-induced activation of the BSCs' AHA2 in a similar way to BL activation of the GCs' AHA (Hayashi et al., 2017).

Light induces the increase of BSCs' membrane water permeability, K_{leaf} and K_{ros}

Here, we report that in addition to external (experimentally imposed and constant) low pH, light also increases the P_f of isolated BSCs (Figure 8). Evidence is accumulating that P_f level reflects the underlying activity of aquaporins. For example, frog oocytes expressing *AtPIP2;1* had higher P_f induced by co-expressing two of the Arabidopsis 14-3-3 protein isoforms which bound to the AtPIP2;1 (Prado et al., 2019). Thus, it would be tempting to speculate that light increased the BSCs' P_f (Figure 8) by enhancing the activity of one or more of the 11 BSCs' aquaporins (Supplemental Table S2).

Alternatively, or in addition, the light-induced increase in BSC P_f could be due to the alkalization of the BSCs' cytosol (Figure 5B), sensed by a histidine (His 197, conserved in all Arabidopsis PIP aquaporins; assayed in AtPIP2;2; Tournaire-Roux et al., 2003) and a leucine (Leu206 in BvPIP2;2 Fortuna et al., 2019) in the cytosol-facing D loop of the aquaporin protein. Moreover, the concurrent hyperpolarization of BSCs by BL (Figure 5A) could perhaps also contribute to the activation of the BSCs' aquaporins, as suggested by in silico simulations (Hub et al., 2010).

The role of aquaporins in controlling K_{leaf} was identified previously [in walnut, Ben Baaziz et al., 2012; in grapevine (*Vitis vinifera*), Vitali et al., 2016; in poplar (*Populus trichocarpa*), Muries et al., 2019; in Arabidopsis BSCs, Prado et al., 2013; Sade et al., 2014]. In particular, Prado et al. (2019) demonstrated a contribution of the abundant—also in the leaf veins—aquaporin AtPIP2;1 to the diurnal and circadian rhythms of the hydraulic conductance of the Arabidopsis rosette, K_{ros}, which peaked before midday. Thus, in addition to the likely P_f-promoting effect of the slightly acidic pH (6) perfusion solution (a link established by Grunwald et al., 2021), that Prado et al. (2019) used for their K_{ros} measurements, the changes that they observed in K_{ros} also reflected the effects of light and circadian rhythms (Prado et al., 2019). In particular, the circadian regulation of AtPIP2;1 by its protein–protein interaction with a 14-3-3 protein (Prado et al., 2019), which resembles the multitude of protein–protein interactions regulating mammalian aquaporins (reviewed by Roche and Törnroth-Horsefield, 2017), suggests an additional possibility of BL regulation of the BSCs' aquaporins: directly via a protein–protein interaction with the phots.

BL signaling increases the K_{leaf}—a model

Whatever the exact underlying molecular mechanism, our results support the following model of K_{leaf} increase by BL, in a GC-like, BL signal transduction pathway: the BSCs' phot1 and phot2 perceive the BL, which, via BLUS1 and unknown downstream protein kinases (the first of which could perhaps be BHP; Hayashi et al., 2017; Hosotani et al., 2021) activates the plasma membrane H^+-ATPase (AHA2), resulting in the hyperpolarization of the BSC, the alkalization of the BCSs' cytosol and the acidification of the xylem sap, leading to an increase in the BSCs' P_f and a subsequent increase in K_{leaf}.

Expressed schematically:

BL → activation of BSC *phots* → phosphorylation[a] & activation of BLUS1 and downstream kinases → activation of BSC H^+-ATPase (AHA2) → hyperpolarization and cytosol alkalization of BSCs and acidification of xylem sap → increase of P_f of BSCs → K_{leaf} increase

[a]We hypothesize that the abovementioned phosphorylation steps are similar to those seen in GCs (Figure 9), but this has yet to be explored in BSCs.

An early K_{leaf} response to BL—what is the advantage?

Both the opening of the stomata and the increase in K_{leaf} occur in the early morning hours (e.g. Brodribb and Holbrook, 2004; Domec et al., 2009; Locke and Ort, 2015) when the irradiance spectrum includes relatively high levels of BL (Chiang et al., 2019; Matthews et al., 2020, and references therein). What is the advantage of the early [blue-]light response of stomata? We suggest that it allows the acquisition of CO_2 under sub-maximum vapor pressure deficit (VPD, a measure of the driving force for leaf water evaporation), thereby increasing water-use efficiency.

Interestingly, K_{leaf} responds to light even faster than g_s does (Guyot et al., 2012)—in an ultimate manifestation of the independence of the BSCs' BL signal transduction from that of the GCs'. One possible advantage of this almost simultaneity is matching the stomatal opening with the increased water flux into the leaf. Were it not for this accompanying K_{leaf} increase, the BL-induced stomata opening, which peaks in the morning hours (the "golden hour"; Gosa et al., 2019), could lead to an imbalance in leaf water, even in the presence of a relatively low VPD, leading to a drop in the Ψ_{leaf}, which, in turn, could close the stomata

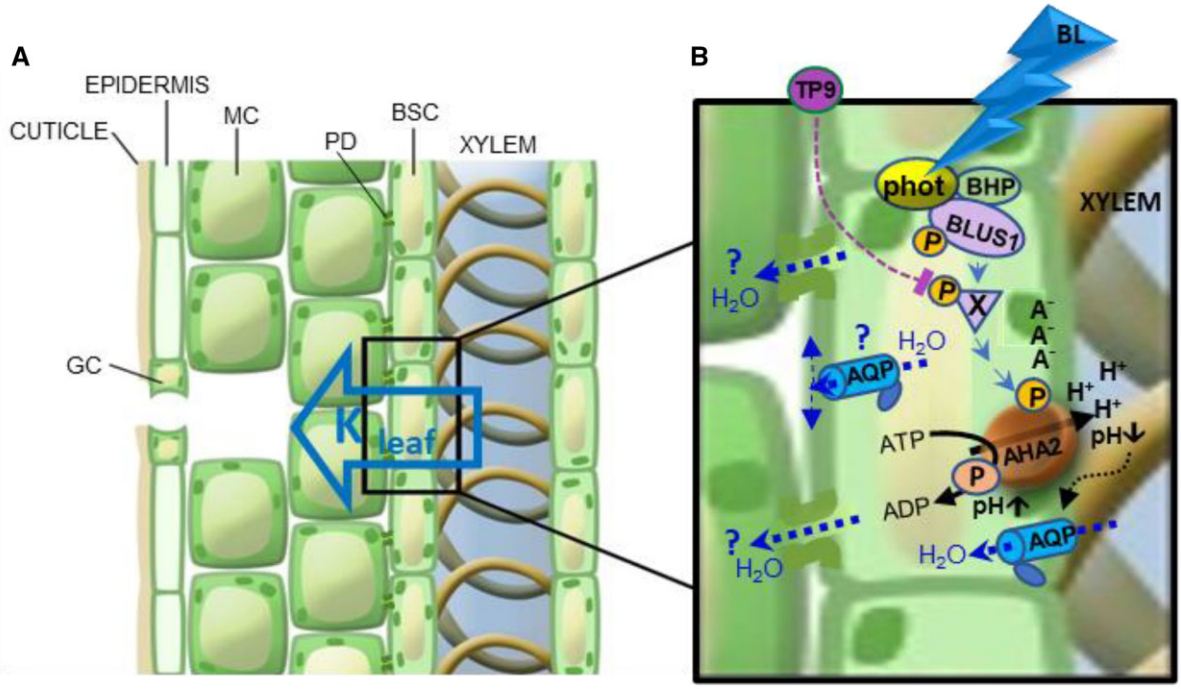

Figure 9 Proposed BSC-autonomous BL signal transduction pathway regulating K_{leaf}, the leaf hydraulic conductance—an artist's rendering. A, A leaf radial water path, from xylem to mesophyll (hollow blue arrow), via the BSCs, which tightly envelop the xylem. MC, mesophyll cell; PD, plasmodesma. B, BL signaling pathway (blue arrowheads) in a BSC, from BL perception by the phototropin receptors (phot) complexed with the kinases, BLUS1 and BHP (Hayashi et al., 2017; Inoue and Kinoshita, 2017), through a hypothesized intermediate TP9-inhibitable phosphorylation (P) of an unknown substrate X by an unknown Raf-like kinase, down to the ultimate AHA2 activation by its phosphorylation (P). AHA2 activation results in proton extrusion via the pump, hyperpolarization (charge separation across the membrane: A^-/H^+), cytosolic alkalinization (pH↑) and xylem sap acidification (pH; also reported in Grunwald et al., 2021), presumably, at the expense of ATP breakdown to ADP with a transient phosphorylation (P) of the catalytic site on the pump protein, as expected from a P-type H^+-ATPase. Xylem sap acidification enhances (black dotted arrow) water permeability (blue dotted arrows) of the BSC's plasma membrane. This is presumably due to enhanced permeability of aquaporins (AQP)s and underlies the increased P_f (osmotic water permeability) of the single BSC and, in turn, also the increased K_{leaf} (Grunwald et al., 2021). P_f in a "constant external pH" may be further increased by light (Figure 8), due to, among other possibilities, cytosolic alkalinization (Figure 5B), and/or the AHA2-generated hyperpolarization (Figure 5A), or, perhaps, even protein–protein interaction with the phots (these possibilities are not represented here). Additional details can be found in the text. Water exiting the BSC via PD between BSCs and the neighboring MCs or via AQPs to the apoplast (blue dotted arrows and question marks) are included for completeness, although it is currently unknown to what extent these symplastic and apoplastic paths contribute to the radial water flow across the BSCs and whether they are also affected by BL.

(Raschke, 1970; Guyot et al., 2012; Klein, 2014; Scoffoni et al., 2018) and thereby limit photosynthesis. Instead, an early morning increase in K_{leaf} elevates Ψ_{leaf}, thereby increasing and prolonging stomatal opening (Raschke, 1970; Guyot et al., 2012; Klein, 2014; Scoffoni et al., 2018). Hypothetically, under more extreme conditions (e.g. with high VPD even in the early morning), BL-increased K_{leaf} would prevent a hydraulic pathway failure when g_s is at its peak (Brodribb and Holbrook, 2004; Halperin et al., 2017; Gosa et al., 2019).

Another possible advantage of the early morning, BL-induced increase in K_{leaf} may be an increased CO_2 permeability of aquaporins. A few lines of evidence converge to support this hypothesis: (1) CO_2 can cross cell membranes through aquaporins, particularly aquaporins of the PIP1 family (Kaldenhoff and Fischer, 2006); (2) the transcripts of PIP1 family aquaporins in walnut have been shown to be upregulated concomitantly with the increase in K_{leaf} induced by a brief (15 min) exposure to WL (Ben Baaziz et al., 2012); (3) in soybean (*Glycine max*), the transcript of a PIP1 family aquaporin (PIP1;8) was found to be more abundant in the morning than at midday, corresponding with a higher K_{leaf} in the morning (Locke and Ort, 2015); (4) aquaporins control K_{leaf} (Shatil-Cohen and Moshelion, 2012; Sade et al., 2014); and (5) CO_2 transported by xylem from the roots may be a source for the CO_2 assimilated into the bundle sheath and mesophyll (Janacek et al., 2009; Hubeau et al., 2019). Thus, assuming the K_{leaf} increase with the first light of day parallels the increase in the permeability of BSC aquaporins to CO_2, the passage from the xylem to the mesophyll of the root-originated CO_2 will be enhanced even before full stomatal opening. The increased availability of CO_2 at this time, when the photosynthetic light is already sufficient, would enhance CO_2 assimilation—a great advantage for the plant. This hypothesis is strengthened by the fact that (Stutz and Hanson, 2019) have shown that the xylem-transported CO_2 constitutes a varying proportion of the total CO_2

assimilated throughout the day depending on the availability of light and CO_2. Notably, photosynthetic CO_2 uptake reaches a maximum within 10 min of exposure to BL (Doi et al., 2015), which is over three-fold faster than the full opening of stomata (Grondin et al., 2015).

The advantage of diminished AHA activity and P_f at night

The fact that the BSC P_f is low in the dark (Figure 8) may explain how the mesophyll does not get flooded at night when root pressure increases. At night, the P_f and K_{leaf} reduction likely prevent water influx into the leaf, while the buildup of root pressure is relieved via guttation. A malfunction of this mechanism is perhaps what underlies leaf flooding by the xylem sap (Shatil-Cohen and Moshelion, 2012). The inactivity of the BSCs' H^+-ATPases, manifested here in the nightly alkalization of the xylem sap and in guttation drops (as noted earlier, for example, also in tomatoes (*Solanum lycopersicum*; Urrestarazu et al., 1996) and poplars (Aubrey et al., 2011), could be advantageous for the plant as a means of energy conservation, as ATPases operate at a high energetic cost (Palmgren, 2001).

Our findings expand the understanding of the molecular basis of the regulation of leaf water influx. The fact that BL increases K_{leaf} in several other species imparts an even more general importance to our results. A focus on the hydraulic valve in series with the stomata should provide new directions for the study of plant water relations in different environments.

Materials and methods

Plant material

Plant genotypes

We used WT *Arabidopsis thaliana* plants ecotype Colombia-0 (Col-0; aka Col), the T-DNA insertion AHA2 mutants *aha2-4* (SALK_ 082786) (Col) and *aha2-4* complemented with *SCR: AHA2* (line 56) (Col), and *SCR:GFP* (Col) as described previously (Grunwald et al., 2021). In addition, we used WT Arabidopsis (Col) with the glabrous mutation (WT Col-gl), *phot1-5* (*nph1-5*) (Col-gl), *phot 2-1* (*npl1-1* or *cav1-1*) (Col-gl), and the double mutant *phot1-5 phot2-1* (*nph1-5 npl1-1*) (Col-gl) (Kagawa et al., 2001), which were kindly provided by the Ken-Ichiro Shimazaki lab (Tokyo, Japan). The *blus1-4* (Col) seed was a kind gift from the Takemiya lab (Yamaguchi, Japan).

Construction of SCR:amiR-PHOT1 plants

The premiR-*PHOT1* or premiR-*PHOT2* and synthetic genes were synthesized by Hylabs (Rehovot, Israel), based on a premiR164 backbone (Alvarez et al., 2006). We used the Web-based MicroRNA Designer (WMD, http://wmd3.weigelworld.org) to produce a premiRNA gene MIR319a as described in WMD. After sequence verification, the premiR-*PHOT1* or premiR-*PHOT2* was cloned into the pDONR 221 and the SCR promoter into pDONRP4P1r (Invitrogen, Waltham, MA, USA) vectors, which are Gateway compatible by BP reactions, and later cloned into the pB7M24GW (Invitrogen) two-fragment binary vector using an LR r reaction, according to the manufacturer's instructions. Each binary vector was transformed into *Agrobacterium tumefaciens* by electroporation and transformed into WT Col-0 using the floral-dip method (Clough and Bent, 1998). Transformants were selected based on their resistance to BASTA herbicide (glufosinate ammonium, Sigma, St Louis, MO, USA; cat. # 45520), grown on plates with Murashige and Skoog (Duchefa, Haarlem, Netherlands; cat. # M222.0050) basal medium + 1% sucrose and 20-μg/mL BASTA. DNA insertion was verified in selected lines by PCR targeting the junction of the premiR-gene and the 35S terminator with the forward primer located ∼1,000 bp from the 3′-end of premiR-gene and reverse primer on the 35S terminator (see primer list in Supplemental Table S1). PCR (polymerized chain reaction) fragments were then sequenced and verified.

Construction of SCR: PHOT1 plants

Binary vectors were constructed with the *PHOT1* gene as described above and then transformed into *phot1-5* (Col-gl1) plants. Successful transformation was verified by PCR.

Plant growth conditions

Plants were grown in 250-mL pots, 2–3 plants per pot filled with soil (Klasmann686, Klasmann-Deilmann, Germany) + 4 g/L Osmocote 6 M in a growth chamber kept at 22°C and 70% relative humidity, with an 8-h light (9:00 am to 5:00 pm)/16-h dark photoperiod. During the day, the illumination, humidity and VPD changed in a pattern resembling natural conditions, as in (Negin and Moshelion, 2017). The illumination intensity provided by LED lights strips [EnerLED 24 V-5630, 24 W/m, 3,000 K (50%)/6,000 K (50%)] reached 150–200 μmol m^{-2} s^{-1} light at the plant level at midday. The plants were irrigated twice a week.

Determination of gas exchange, E and gs, and hydraulic conductance, K_{leaf}

Preparation of detached leaves for gas-exchange measurements

Fully expanded leaves from 7- to 8-week-old plants were excised at the petiole base using a wet, sharp blade under a drop of water. Petioles were immediately submerged in 0.5-mL Eppendorf tubes with AXS (3-mM KNO_3, 1-mM $Ca(NO_3)_2$, 1-mM $MgSO_4$, 3-mM $CaCl_2$, 0.25-mM NaH_2PO_4, 90-μM EDFS (Ethylenediaminetetraacetic acid ironIII sodium salt) (Sigma)]. The leaves were excised, shortly before the "lights off" transition (around 5:00 pm) on the evening preceding the measurements and placed in gas-sealed, transparent 25 × 20 × 15 cm plastic boxes with water-soaked tissue paper on the bottom to provide ∼90% humidity. The transparent boxes were then inserted into a larger light-proof plastic box overnight and kept in total darkness until the start of light treatments the next morning.

Light treatments of detached leaves

All gas-exchange experiments were conducted in a dark room (<1 umol m^{-2} s^{-1}) at a constant temperature of 22°C, between 10:00 am and 1:00 pm. The excised leaves were taken out of the light-sealed box and placed in one of two custom-made light chambers. The total illumination intensity in both light chambers was set to roughly 220 µmol m^{-2} s^{-1}. In the RL chamber, the leaves were illuminated only with RL (660 nm) and in the RL + BL chamber they were illuminated with ∼90% RL and 10% BL (450 nm). Leaves were exposed to either RL or RL + BL for 15 min at an ambient VPD of 1.3–1.5 kPa. A fan circulated the air in each light chamber for uniform and constant temperature and VPD. Next, leaves were transferred to an LI-COR 6400XT for an additional 2–3 min, under the same illumination conditions with VPD of ∼1.3 kPa, until stabilization of the gas-exchange measurements, after which a measurement was recorded. D-LED lighting with adjustable current source (DR-SD6/12) was used as light sources (http://www.d-led.net/). Light intensity was verified daily using an LI-250A light meter with an LI-190SA quantum sensor (LI-COR, Lincoln, NE, USA).

Measurements of gas exchange, E and g_s, and hydraulic conductance, K_{leaf}

Following the light treatments, the leaves were immediately placed in an LI-COR 6400XT for measurements of stomatal conductance (g_s) and transpiration (E) similar to Grunwald et al. (2021), with the following changes: all of the experiments were conducted in the dark at 22°C and the illumination in the LI-COR cuvette was adjusted to match the preceding light treatments. Then, the water potential (Ψ_{leaf}) was determined in a pressure chamber (ARIMAD-3000; MRC Israel) and K_{leaf} was calculated (as in Grunwald et al., 2021) as:

$$K_{leaf} = -E/(\Psi_{leaf} - \Psi_{AXS})_{\approx} - E/\Psi_{leaf} \quad (1)$$

Additionally, g_s was measured at the same time as above using LI-COR 6400XT on intact leaves of whole plants left under the growth-room illumination for 2–4 h after the lights were turned on. Illumination settings in the instrument's cuvette were set to the same conditions as in the growth room.

Inhibition of light transduction in detached leaves

TP9 (ENZO, Farmingdale, NY, USA; cat. # BML-EI21, 100 mM in DMSO (Sigma; cat. # W387520), kept in aliquots at −18°C) was added to the AXS to a final concentration of 10 µM. AXS with DMSO at a concentration of 100 µL/L (vol/vol) served as a control in this set of experiments. Excised leaves were kept overnight until the measurements were made as described above. For surface application, 0.05% (vol/vol) Tween-20 (J.T. Baker, Phillipsburg, NJ, USA; cat. # X251-07) was added to the TP9 and control solutions and sprayed prior to overnight perfusion with unmodified AXS. Boxes holding the sprayed leaves did not contain the damp tissue paper, and leaves were patted dry prior to placing them in the light chamber to ensure the leaf surface was dry when the leaves were placed in the LI-COR 6400xt cuvettes.

Determination of xylem sap pH in detached leaves

Leaf preparation for imaging

On the eve of the experiment, leaves from 6- to 7-week-old plants, ∼2.5-cm long and 1-cm wide, were excised with a sharp blade and perfused (as described) with AXS containing 100 µM of the dual-excitation fluorescent pH probe, (fluorescein isothiocyanate conjugated to 10 kDa dextran (Sigma; cat. # FD10S), added from a 10-mM stock in double-distilled water). The excised leaves were then placed in the "double box" setup (i.e. a sealed plastic box inside a dark box) and kept in the dark until measurements the next morning.

Dark-treated leaves: Leaves were taken out of the dark boxes and immediately prepared for vein imaging on a microscope slide under low-light conditions (<5 µmol m^{-2} s^{-1}).

Light-treated leaves: Leaves were taken out of the dark boxes and placed in the growth chamber inside transparent gas sealed boxes (boxes as in K_{leaf}) for 30 min of growth room WL illumination (see above under "Plant growth conditions") and were subsequently imaged.

Image capture and analysis

The leaves were imaged using an inverted microscope (Olympus-IX8, as detailed by Grunwald et al., 2021). Image capture and image analysis of the intra-xylem pH were as already described (Grunwald et al., 2021).

Determination of the BSCs' membrane potential (E_M)

Protoplast preparation

To evaluate the protoplast membrane potential (E_M), we used a fluorescent (E_M-sensitive dual-excitation ratiometric dye, di-8-ANEPPS (Pucihar et al., 2009), and an inverted epi-fluorescence microscope (Eclipse Ti-S, Nikon, Tokyo, Japan) coupled to an IXON Ultra 888 camera (Andor, UK). A Nikon 40× objective (Plan Fluor 40x/0.75, OFN25 DIC M/N2) was used for protoplast viewing and imaging. The experiments were performed between 10 am and 4 pm. BSC protoplasts were isolated as described (Shatil-Cohen et al., 2014) from 6- to 8-week-old SCR:GFP (Col) plants and kept in an Eppendorf vial at room temperature (22°C ± 2°C) in the dark until use. A drop with a few protoplasts was added to a bath solution in an experimental chamber, containing 30-µM di-8-ANEPPS and 0.05% (vol/vol) pluronic acid, with or without 10-µM TP9 (see "Solutions" below), and protoplasts were allowed to settle for 10 min on a glass coverslip bottom. In separate control assays, we verified the viability of the TP9-treated cells by observing that they remained capable of de-esterifying (hydrolyzing) the accumulated

SNARF1-AM (see below) and retaining the fluorescent form of the dye, SNARF1, in the cytoplasm.

GFP-based selection

An individual, perfectly round BSC (25-to 32.5-μm diameter) was selected for imaging based on its GFP (green fluorescenct protein) fluorescence (excitation of 490/15 nm) delivered by a xenon lamp monochromator, Polychrome II (Till Photonics, Munich, Germany), under the control of IW6.1 (Imaging Workbench 6.1) software (Indec Biosystems, Santa Clara, CA, USA), and the emitted fluorescence was filtered via a 515 nm dichroic mirror and a 525/50-nm band-pass barrier filter.

Size-based selection

In a single set of experiments, we used a *phot1-5* (Col-gl) mutant and WT (Col-gl) plants that were not labeled with GFP. BS protoplasts are ∼50% smaller than mesophyll cells and contain about half as many chloroplasts as mesophyll cells (Shatil-Cohen et al., 2011) and are relatively easy to detect under transmitted light. Thus, we based the BSC selection on rejecting as "non-BSCs" protoplasts outside the above-mentioned size range (25- to 32.5-mm diameter). In a separately conducted experiment on protoplasts from GFP-labeled WT (Col), such size-based guesses were confirmed by GFP fluorescence in 68 out of 101 cases.

Light treatments and imaging

The selected BSC protoplast in the experimental chamber was exposed to the dark for 10–20 min (control), and a first pair of di-8-ANEPPS fluorescence images was recorded (excitation by a pair of 50 ms pulses, 438 nm then 531 nm, 3 ms apart, was delivered by the Polychrome II; the emitted fluorescence was filtered via a dichroic mirror of 570 nm and 585/20-nm emission band-pass filter; Chroma Technology Corp., Bellows Falls, VT, USA). Subsequently, the protoplast was illuminated for 5–10 min (by a home-made illuminator of crystal clear LEDs from Tal-Mir Electronics, Israel) with either RL (660 nm, 220 μmol m^{-2} s^{-1}) or RL + BL (BL: 450 nm, 10%–15% of the total intensity of 220 μmol m^{-2} s^{-1}) and a second pair of fluorescence images was recorded as above. The images were processed using FIJI (Abràmoff et al., 2004; Schindelin et al., 2012) to yield a pixel-by-pixel fluorescence ratio, as described previously (Wigoda et al., 2017).

Fluorescence ratio calibration

BSC protoplasts incubated in di-8-ANEPPS as above were subjected to 5-s-long voltage pulses in the range of + 17 to −223 mV using a patch-clamp pipette in a whole-cell configuration. A pair of images was recorded during the second half of each pulse, at a steady state. The patch-clamp imaging setup was as described in detail by Wigoda et al. (2017), except for the substitution of the abovementioned Eclipse microscope and IXON camera for the original image-acquisition instruments. This calibration confirmed the previously published positive correlation between the di-8-ANEPPS fluorescence ratio and depolarization (Supplemental Figure S6). This definitively positive correlation allows us to draw a clear conclusion about the direction of the experimentally induced change in the E_M, even if the relatively wide data distribution suggests caution in accepting the absolute E_M values.

Solutions

Di-8-ANEPPS (Molecular Probes/Thermo Fisher Scientific; cat. # D3167, Oregon, USA): a 10-mM stock solution in DMSO (dimethyl sulfoxide) was stored in 10-μL aliquots at −20°C.

Pluronic F-127 (Molecular Probes/Thermo Fisher Scientific, cat. # P6867, Oregon, USA), a 20% stock solution in DMSO was stored in 100-μL aliquots at room temperature.

Bath solution (millimolar): 5 KCl, 1 $CaCl_2$, 4 $MgCl_2$, and 10 MES; pH 5.6; osmolality: 435 mOsm, adjusted w/D-sorbitol.

Patch-clamp pipette solution (millimolar):112 K-gluconate, 28 KCl, 2 $MgCl_2$, 10 HEPES, and 328 sorbitol; pH 7.5. Osmolarity: 480 mOsm.

TP9 was added to the bath solution from aliquots used in the detached leaves experiments.

Determination of the BSCs' pH_{CYT}

The experiments were performed between 10 am and 4 pm. BSC protoplasts were isolated according to Shatil-Cohen et al. (2014) from 6- to 8-week-old SCR:GFP (Col) plants and kept in an Eppendorf vial at room temperature (22 ± 2°C) in the dark until use. The protoplasts were treated as described previously (Torne-Srivastava et al., 2021), with the following modifications: a 10- min treatment was applied, either dark or RL + BL or RL (the illumination setting was as described above for E_M determination), the bath solution was used for flushing out the external SNARF1-AM during the last 1 min of the dark/light treatments and the cells were imaged within the subsequent 5 min. Image acquisition and analysis to determine the pH_{CYT} values were performed as described previously (Torne-Srivastava et al., 2021).

Solutions

Bath solution for protoplasts' pH_{CYT} determination: as for E_M determination.

SNARF1-AM: Carboxy seminaphthorhodafluor-1, acetoxymethyl ester, acetate (Molecular Probes, Thermo Fisher cat. #: C-1272); a 50- μg prepackaged portion was dissolved into a 10-mM stock in DMSO, and then stored in 10-μL aliquots at −20°C.

Pluronic F-127: as for E_M determination.

Measuring leaf vein density

Vein density was measured as described previously (Grunwald et al., 2021).

Determination of the osmotic water permeability coefficient (P_f) under different light regimes

Protoplast isolation and P_f determination

These experiments were performed on *SCR:GFP* (Col) protoplasts as described previously (Shatil-Cohen et al., 2014; Grunwald et al., 2021), with minor modifications of

equipment and protocol listed in the latter. The P_f value was extracted from the image analysis of the rate of the videotaped protoplast challenged with a hypotonic solution, and a simultaneous fit of the swelling time course and the time course of the osmotic concentration change in the bath (C_{out}) during the hypotonic challenge. The latter was reconstructed from the videotaped rate of change of optical density of a solution of black ink dissolved in the hypotonic solution flushed into the experimental bath in a separate experiment (Moshelion et al., 2004; Shatil-Cohen et al., 2014; Grunwald et al., 2021).

After their isolation, the protoplasts were divided into two: the "light-treated" protoplasts were kept in a vial under the lights of the growth chamber for the duration of the experiment (between 10 am and 2 pm), the "dark-treated" protoplasts were kept in a vial in a light-proof box. The two types were sampled alternatingly preserving their respective conditions of illumination (using green safe light while sampling in the dark). The sampled "light-treated" protoplasts were placed in the experimental chamber and left to settle down for 10–40 min on the bench under a cool-white-led illumination, and then, for 5–7 min on the microscope stage under the unfiltered microscope light (6 V/30 W halogen lamp, PHILIPS 5761) during preparations and the 1 min videotaping of swelling during the osmotic challenge. The sampled "dark-treated" protoplasts were placed, under green "safe light," in the experimental chamber, left to settle for ~10 min and after the brief location of a GFP-positive BSC they remained in total darkness for 10 min. The 1-min videotaping of the protoplast's swelling during the hypoosmotic challenge in the dark necessitated an illumination by the microscope lamp filtered (to block out the BL) via a red plastic band-pass filter (~600–700 nm/30 μmol m^{-2} s^{-1}).

Determination of the pH of guttation drops

Whole, intact WT (Col) plants were covered overnight with black plastic bags to increase the relative humidity in their atmosphere and to prevent E. The following morning, immediately after the growth room lights went on, guttation droplets were collected from the tips of the leaves. Ten to 20 guttation droplets were collected and pooled to reach a sample volume of ~20 μL in a 200-μL vial, which was immediately sealed. pH was measured within 10 min of sample collection using a micro-pH electrode MI-410 (Microlectrode, Inc., Bedford, NH, USA).

Graphics and statistics

The Box plots were drawn using ORIGIN (OriginPro, Version 2022. OriginLab Corporation, Northampton, MA, USA). The statistical analyses were performed using JMP (JMPPro, Version 16.0.0 (512257), SAS Institute Inc., Cary, NC, USA, 1989–2021). For significance and *P*-values, please see supplemental statistical data.

Accession numbers

Please refer to Supplemental Table S2 for all accession numbers and full gene details.

Supplemental data

The following materials are available in the online version of this article.

Supplemental Figure S1. phot receptor mutants do not show any effect of BL on their g_s, E, or Ψ_{leaf}.

Supplemental Figure S2. *SCR:amiR*-silencing of the *PHOT1* or *PHOT2* genes in the BSCs reduces Ψ_{leaf} under RL + BL, but does not reduce the stomatal conductance (g_s) or the rate of transpiration (E).

Supplemental Figure S3. BSC-directed *PHOT1* complementation of the *phot1-5* mutant elevates the Ψ_{leaf}, but not stomatal conductance (g_s), or the transpiration rate (E).

Supplemental Figure S4. TP9 perfused via the petiole does not affect the examined physiological parameters under RL-only illumination.

Supplemental Figure S5. Xylem-fed kinase inhibitor TP9 does not affect the BL-induced increase in the transpiration rate (E), but does prevent any BL-induced increase in Ψ_{leaf}.

Supplemental Figure S6. The relationship between the di-8-ANEPPS fluorescence ratio (F-ratio, F438/F531) and the BSC membrane potential (EM).

Supplemental Figure S7. BSC-directed AHA2 complementation of the aha2-4 mutant restores its BL-induced Ψleaf increase, but not the BL-induced increases in stomatal conductance (g_S) or in the transpiration rate (E).

Supplemental Figure S8. Leaf vein density does not depend on the expression of phot1 or phot2.

Supplemental Figure S9. After prolonged illumination, stomatal conductance (g_s) of intact leaves of whole plants did not differ among the different genotypes (WT, *phot* mutants, and *phot1-5* complemented with *SCR:PHOT1*).

Supplemental Figure S10. The BLUS1 kinase mutation abolishes the BL-induced Kleaf increase.

Supplemental Figure S11. The hyperpolarization of BSC protoplasts by BL is prevented by the phot1 mutation.

Supplemental Statistical Data Set 1. Statistical information.

Supplemental Table S1. List of primers used in this study.

Supplemental Table S2. Expression levels of some genes found in the transcriptomes of BSCs and mesophyll (MES) cells (Wigoda et al., 2017, GEO repository Experiment GSE85463) that are or may be related to BL signaling, encoding receptors, kinases, H^+-ATPases, and aquaporins.

Acknowledgments

We thank Dr. Dizza Bursztyn of the Hebrew University of Jerusalem for assisting us with the statistical analysis of this work. We thank Dr Naama Gil and Dr Idan Efroni for assisting in the RLM RACE *amiRNA* procedure.

Funding

This research was supported by the Israel Science Foundation (ISF) grant No. 1043/20 to M.M. and the ISF grant No. 1312/12 to N.M.

Conflict of interest statement. None declared.

References

Aasamaa K, Sõber A (2012) Light sensitivity of shoot hydraulic conductance in five temperate deciduous tree species. Funct Plant Biol **39**: 661

Abràmoff MD, Magalhães PJ, Ram SJ (2004) Image processing with imageJ. Biophotonics Int **11**: 36–41

Alvarez JP, Pekker I, Goldshmidt A, Blum E, Amsellem Z, Eshed Y (2006) Endogenous and synthetic microRNAs stimulate simultaneous, efficient, and localized regulation of multiple targets in diverse species. Plant Cell **18**: 1134–1151

Assmann S (1993) Signal transduction in guard cells. Annu Rev Cell Dev Biol **9**: 345–375

Assmann SM, Simoncini L, Schroeder JI (1985) Blue light activates electrogenic ion pumping in guard cell protoplasts of Vicia faba. Nature **318**: 285–287

Aubrey DP, Boyles JG, Krysinsky LS, Teskey RO (2011) Spatial and temporal patterns of xylem sap pH derived from stems and twigs of Populus deltoides L. Environ Exp Bot **71**: 376–381

Ben Baaziz K, Lopez D, Rabot A, Combes D, Gousset A, Bouzid S, Cochard H, Sakr S, Venisse JS (2012) Light-mediated Kleaf induction and contribution of both the PIP1s and PIP2s aquaporins in five tree species: walnut (Juglans regia) case study. Tree Physiol **32**: 423–434

Brodribb TJ, Holbrook NM (2004) Diurnal depression of leaf hydraulic conductance in a tropical tree species. Plant Cell Environ **27**: 820–827

Chiang C, Olsen JE, Basler D, Bånkestad D, Hoch G (2019) Latitude and weather influences on sun light quality and the relationship to tree growth. Forests **10**: 610

Clough SJ, Bent AF (1998) Floral dip: a simplified method for Agrobacterium-mediated transformation of *Arabidopsis thaliana*. Plant J **16**: 735–743

Den Os D, Staal M, Elzenga JTM (2007) Signal integration by ABA in the blue light-induced acidification of leaf pavement cells in pea (Pisum sativum L. var. Argenteum). Plant Signal Behav **2**: 146–152

Doi M, Kitagawa Y, Shimazaki KI (2015) Stomatal blue light response is present in early vascular plants. Plant Physiol **169**: 1205–1213

Domec JC, Noormets A, King JS, Sun G, McNulty SG, Gavazzi MJ, Boggs JL, Treasure EA (2009) Decoupling the influence of leaf and root hydraulic conductances on stomatal conductance and its sensitivity to vapour pressure deficit as soil dries in a drained loblolly pine plantation. Plant Cell Environ **32**: 980–991

Elmore JM, Coaker G (2011) The role of the plasma membrane H + -ATPase in plant–microbe interactions. Mol Plant **4**: 416–427

Fortuna CA, Zerbetto De Palma G, Aliperti Car L, Armentia L, Vitali V, Zeida A, Estrin DA, Alleva K (2019) Gating in plant plasma membrane aquaporins: the involvement of leucine in the formation of a pore constriction in the closed state. FEBS J **286**: 3473–3487

Gosa SC, Lupo Y, Moshelion M (2019) Quantitative and comparative analysis of whole-plant performance for functional physiological traits phenotyping: new tools to support pre-breeding and plant stress physiology studies. Plant Sci **282**: 49–59

Grondin A, Rodrigues O, Verdoucq L, Merlot S, Leonhardt N, Maurel C (2015) Aquaporins contribute to ABA-triggered stomatal closure through OST1-mediated phosphorylation. Plant Cell **27**: 1945–1954

Grunwald Y, Wigoda N, Sade N, Yaaran A, Torne T, Gosa SC, Moran N, Moshelion M (2021) Arabidopsis leaf hydraulic conductance is regulated by xylem sap pH, controlled, in turn, by a P-type H + -ATPase of vascular bundle sheath cells. Plant J **106**: 301–313

Guyot G, Scoffoni C, Sack L (2012) Combined impacts of irradiance and dehydration on leaf hydraulic conductance: insights into vulnerability and stomatal control. Plant Cell Environ **35**: 857–871

Halperin O, Gebremedhin A, Wallach R, Moshelion M (2017) High-throughput physiological phenotyping and screening system for the characterization of plant-environment interactions. Plant J **89**: 839–850

Hayashi M, Inoue S, Ueno Y, Kinoshita T (2017) A Raf-like protein kinase BHP mediates blue light-dependent stomatal opening. Sci Rep **7**: 45586

Hosotani S, Yamauchi S, Kobayashi H, Fuji S, Koya S, Shimazaki K, Takemiya A (2021) A BLUS1 kinase signal and a decrease in intercellular CO2 concentration are necessary for stomatal opening in response to blue light. Plant Cell **33**: 1813–1827

Hub JS, Aponte-Santamaría C, Grubmüller H, De Groot BL (2010) Voltage-regulated water flux through aquaporin channels in silico. Biophys J **99**: L97–L99

Hubeau M, Thorpe MR, Mincke J, Bloemen J, Bauweraerts I, Minchin PEH, De Schepper V, De Vos F, Vanhove C, Vandenberghe S, et al. (2019) High-resolution in vivo imaging of xylem-transported CO2 in leaves based on real-time 11C-tracing. Front For Glob Chang **2**: 25.

Inoue S, Kinoshita T (2017) Blue light regulation of stomatal opening and the plasma membrane H $^{+}$ -ATPase. Plant Physiol **174**: 531–538

Janacek SH, Trenkamp S, Palmer B, Brown NJ, Parsley K, Stanley S, Astley HM, Rolfe SA, Paul Quick W, Fernie AR, et al.. (2009) Photosynthesis in cells around veins of the C 3 plant *Arabidopsis thaliana* is important for both the shikimate pathway and leaf senescence as well as contributing to plant fitness. Plant J **59**: 329–343

Kaldenhoff R, Fischer M (2006) Aquaporins in plants. Acta Physiol **187**: 169–176

Karlsson PE (1986) Blue light regulation of stomata in wheat seedlings. II. Action spectrum and search for action dichroism. Physiol Plant **66**: 207–210

Kinoshita T, Doi M, Suetsugu N, Kagawa T, Wada M, Shimazaki K (2001) Phot1 and Phot2 mediate blue light regulation of stomatal opening. Nature **414**: 656–660

Kinoshita T, Shimazaki K (1999) Blue light activates the plasma membrane H + -ATPase by phosphorylation of the C-terminus in stomatal guard cells. EMBO J **18**: 5548–5558

Klein T (2014) The variability of stomatal sensitivity to leaf water potential across tree species indicates a continuum between isohydric and anisohydric behaviours. Funct Ecol **28**: 1313–1320

Kronenberg GHM, Kendrick RE (1986) The physiology of action. Photomorphogenesis in Plants. Springer Netherlands, Dordrecht, Netherlands, pp 99–114

Locke AM, Ort DR (2015) Diurnal depression in leaf hydraulic conductance at ambient and elevated [CO2] reveals anisohydric water management in field-grown soybean and possible involvement of aquaporins. Environ Exp Bot **116**: 39–46

Matthews JS, Vialet-Chabrand S, Lawson T, Evans J (2020) Role of blue and red light in stomatal dynamic behaviour. J Exp Bot **71**: 2253–2269

Moshelion M, Moran N, Chaumont F (2004) Dynamic changes in the osmotic water permeability of protoplast plasma membrane. Plant Physiol **135**: 2301–2317

Muries B, Mom R, Benoit P, Brunel-michac N, Cochard H, Drevet P, Petel G, BadelE, FumanalB, Gousset-duponta A, et al. (2019) Aquaporins and water control in drought-stressed poplar leaves: a glimpse into the extraxylem vascular territories. Environ Exp Bot **162**: 25–37

Negin B, Moshelion M (2017) The advantages of functional phenotyping in pre-field screening for drought-tolerant crops. Funct Plant Biol **44**: 107

Palmgren MG (2001) Plant plasma membrane H^{+}ATPases: powerhouses for nutrient uptake . Annu Rev Plant Physiol Plant Mol Biol **52**: 817–845

Prado K, Boursiac Y, Tournaire-Roux C, Monneuse JM, Postaire O, Da Ines O, Schaffner AR, Hem S, Santoni V, Maurel C (2013) Regulation of arabidopsis leaf hydraulics involves light-dependent phosphorylation of aquaporins in veins. Plant Cell **25**: 1029–1039

Prado K, Cotelle V, Li G, Bellati J, Tang N, Tournaire-Roux C, Martinière A, Santoni V, Maurela C (2019) Oscillating aquaporin phosphorylation and 14-3-3 proteins mediate the circadian regulation of leaf hydraulics. Plant Cell **31**: 417–429

Prado K, Maurel C (2013) Regulation of leaf hydraulics: from molecular to whole plant levels. Front Plant Sci **4**: 1–14

Pucihar G, Kotnik T, Miklavčič D (2009) Measuring the Induced Membrane Voltage with Di-8-ANEPPS. J Vis Exp 1659. doi:10.3791/1659

Raschke K (1970) Stomatal responses to pressure changes and interruptions in the water supply of detached leaves of Zea mays L. Plant Physiol **45**: 415–423

Roche J, Törnroth-Horsefield S (2017) Aquaporin protein-protein interactions. Int J Mol Sci **18**: 2255

Roelfsema MRG, Hedrich R (2005) In the light of stomatal opening: new insights into 'the Watergate.' New Phytol **167**: 665–691

Roelfsema MRG, Steinmeyer R, Staal M, Hedrich R (2001) Single guard cell recordings in intact plants: light-induced hyperpolarization of the plasma membrane. Plant J **26**: 1–13

Sade N, Shatil-Cohen A, Attia Z, Maurel C, Boursiac Y, Kelly G, Granot D, Yaaran A, Lerner S, Moshelion M (2014) The role of plasma membrane aquaporins in regulating the bundle sheath-mesophyll continuum and leaf hydraulics. Plant Physiol **166**: 1609–1620

Sakai T, Kagawa T, Kasahara M, Swartz TE, Christie JM, Briggs WR, Wada M, Okada K (2001) Arabidopsis nph1 and npl1: blue light receptors that mediate both phototropism and chloroplast relocation. Proc Natl Acad Sci USA **98**: 6969–6974

Schindelin J, Arganda-Carreras I, Frise E, Kaynig V, Pietzsch T, Longair M, Preibisch S, Rueden C, Saalfeld S, Schmid B, et al. (2012) Fiji: an open-source platform for biological-image analysis. Nat Methods **9**: 676–682

Scoffoni C, Albuquerque C, Cochard H, Buckley TN, Fletcher LR, Caringella MA, Bartlett M, Brodersen CR, Jansen S, Mcelrone AJ (2018) The causes of leaf hydraulic vulnerability and its influence on gas exchange in *Arabidopsis thaliana*. **178**: 1584–1601

Sellin A, Sack L, Õunapuu E, Karusion A (2011) Impact of light quality on leaf and shoot hydraulic properties: a case study in silver birch (Betula pendula). Plant Cell Environ **34**: 1079–1087

Shapira O, Khadka S, Israeli Y, Shani U, Schwartz A (2009) Functional anatomy controls ion distribution in banana leaves: significance of Na + seclusion at the leaf margins. Plant Cell Environ **32**: 476–485

Shatil-Cohen A, Attia Z, Moshelion M (2011) Bundle-sheath cell regulation of xylem-mesophyll water transport via aquaporins under drought stress: a target of xylem-borne ABA? Plant J **67**: 72–80

Shatil-Cohen A, Moshelion M (2012) Smart pipes. Plant Signal Behav **7**: 1088–1091

Shatil-Cohen A, Sibony H, Draye X, Chaumont F, Moran N, Moshelion M (2014) Measuring the osmotic water permeability coefficient (Pf) of spherical cells: isolated plant protoplasts as an example. J Vis Exp (92): e51652

Shimazaki K, Doi M, Assmann SM, Kinoshita T (2007) Light regulation of stomatal movement. Annu Rev Plant Biol **58**: 219–247

Stutz SS, Hanson DT (2019) Contribution and consequences of xylem-transported CO2 assimilation for C3 plants. New Phytol **223**: 1230–1240

Svennelid F, Olsson A, Piotrowski M, Rosenquist M, Ottman C, Larsson C, Oecking C, Sommarin M (1999) Phosphorylation of Thr-948 at the C terminus of the plasma membrane H-ATPase creates a binding site for the regulatory 14-3-3 protein. Plant Cell **11**: 2379–2391

Takemiya A, Sugiyama N, Fujimoto H, Tsutsumi T, Yamauchi S, Hiyama A, Tada Y, Christie JM, Shimazaki KI (2013) Phosphorylation of BLUS1 kinase by phototropins is a primary step in stomatal opening. Nat Commun **4**: 2094

Talbott LD, Shmayevich IJ, Chung Y, Hammad JW, Zeiger E (2003) Blue light and phytochrome-mediated stomatal ppening in the npq1 and phot1 phot2 mutants of Arabidopsis. Plant Physiol **133**: 1522–1529

Torne-Srivastava T, Grunwald Y, Dalal A, Yaaran A, Moran N (2021) Stress is basic: ABA alkalinizes both the xylem sap and the cytosol by inhibiting their P-type H^+-ATPase and stimulating their V-type H^+-ATPase bioRxiv, doi:10.1101/2021.03.24.436813

Tournaire-Roux C, Sutka M, Javot H, Gout E, Gerbeau P, Luu DT, Bligny R, Maurel C (2003) Cytosolic pH regulates root water transport during anoxic stress through gating of aquaporins. Nature **425**: 393–397

Ueno K, Kinoshita T, Inoue S, Emi T, Shimazaki K (2005) Biochemical characterization of plasma membrane H + -ATPase activation in guard cell protoplasts of *Arabidopsis thaliana* in response to blue light. Plant Cell Physiol **46**: 955–963

Urrestarazu M, Sanchez A, Lorente FA, Guzmán M (1996) A daily rhythmic model for pH and volume from xylem sap of tomato plants. Commun Soil Sci Plant Anal **27**: 1859–1874

Vitali M, Cochard H, Gambino G, Ponomarenko A, Perrone I, Lovisolo C (2016) VvPIP2;4N aquaporin involvement in controlling leaf hydraulic capacitance and resistance in grapevine. Physiol Plant **158**: 284–296

Voicu MC, Cooke JEK, Zwiazek JJ (2009) Aquaporin gene expression and apoplastic water flow in bur oak (Quercus macrocarpa) leaves in relation to the light response of leaf hydraulic conductance. J Exp Bot **60**: 4063–4075

Voicu MC, Zwiazek JJ, Tyree MT (2008) Light response of hydraulic conductance in bur oak (Quercus macrocarpa) leaves. Tree Physiol **28**: 1007–1015

Wigoda N, Pasmanik-Chor M, Yang T, Yu L, Moshelion M, Moran N (2017) Differential gene expression and transport functionality in the bundle sheath versus mesophyll – a potential role in leaf mineral homeostasis. J Exp Bot **68**: 3179–3190

Zeiger E, Assmann SM, Meioner H (1983) The photobiology of Paphiopedilum stomata: opening under blue lightbut not red light. Photochem Photobiol **38**: 627–630.

Zeiger E, Helper PK (1977) Light and stomatal function: blue light stimulates swelling of guard cell protoplasts. Science **196**: 887–889